ELSEVIER

Clinical Neurophysiology 114 (2003) 1580–1593

www.elsevier.com/locate/clinph

EMG contamination of EEG: spectral and topographical characteristics

I.I. Goncharova*, D.J. McFarland, T.M. Vaughan, J.R. Wolpaw*

Laboratory of Nervous System Disorders, Wadsworth Center, New York State Department of Health and State University of New York, Empire State Plaza, P.O. Box 509, Albany, NY 12201-0509, USA

Accepted 17 March 2003

Abstract

Objective: Electromyogram (EMG) contamination is often a problem in electroencephalogram (EEG) recording, particularly, for those applications such as EEG-based brain–computer interfaces that rely on automated measurements of EEG features. As an essential prelude to developing methods for recognizing and eliminating EMG contamination of EEG, this study defines the spectral and topographical characteristics of frontalis and temporalis muscle EMG over the entire scalp. It describes both average data and the range of individual differences.

Methods: In 25 healthy adults, signals from 64 scalp and 4 facial locations were recorded during relaxation and during defined (15, 30, or 70% of maximum) contractions of frontalis or temporalis muscles.

Results: In the average data, EMG had a broad frequency distribution from 0 to >200 Hz. Amplitude was greatest at 20–30 Hz frontally and 40–80 Hz temporally. Temporalis spectra also showed a smaller peak around 20 Hz. These spectral components attenuated and broadened centrally. Even with weak (15%) contraction, EMG was detectable ($P < 0.001$) near the vertex at frequencies >12 Hz in the average data and >8 Hz in some individuals.

Conclusions: Frontalis or temporalis muscle EMG recorded from the scalp has spectral and topographical features that vary substantially across individuals. EMG spectra often have peaks in the beta frequency range that resemble EEG beta peaks.

Significance: While EMG contamination is greatest at the periphery of the scalp near the active muscles, even weak contractions can produce EMG that obscures or mimics EEG alpha, mu, or beta rhythms over the entire scalp. Recognition and elimination of this contamination is likely to require recording from an appropriate set of peripheral scalp locations.

Keywords: Electroencephalogram; Electromyogram; Artifact; Brain–computer interface; Rehabilitation

1. Introduction

Contamination of the electroencephalogram (EEG) signal by muscle activity is an old and well-recognized problem for clinical and experimental electroencephalography (Barlow, 1986). Electromyogram (EMG) artifact is of greatest concern for research studies or clinical applications that depend on automatic online detection and measurement of EEG features. EEG-based brain–computer interface (BCI) systems fall into this group. BCI systems allow their users to communicate with others or control devices (such as a simple word-processing program) by controlling specific features of the EEG (Wolpaw et al., (2002) for review). Thus, they require either artifact-free EEG or the capacity to detect artifacts in real-time and prevent them from affecting communication and control. This requirement is particularly important because BCI systems are intended for individuals with severe motor disorders such as amyotrophic lateral sclerosis (ALS) and cerebral palsy that may be associated with frequent involuntary contractions of cranial or facial muscles.

Several present-day BCI systems rely on mu (8–12 Hz) or beta (18–24 Hz) rhythms recorded from the scalp over sensorimotor cortices (e.g. Pfurtscheller et al., 2000; Wolpaw et al., 2000; Kostov and Polak, 2000). Mu- or beta-rhythm amplitudes are translated into cursor movements on a video screen. The system user learns to control these rhythms so as to move the cursor to select a desired item from among a set of choices. Even though these rhythms are typically recorded from central locations, they

* Corresponding author. Tel.: +1-518-486-2677 (I.I. Goncharova), +1-518-473-3631 (J.R. Wolpaw); fax: +1-518-486-4910.

E-mail addresses: gonchar@wadsworth.org (I.I. Goncharova), wolpaw@wadsworth.org (J.R. Wolpaw).

1388-2457/03/$30.00
doi:10.1016/S1388-2457(03)00093-2

might still be obscured by EMG. EMG contamination could be a particular problem for BCI users in whom ALS has led to degeneration of sensorimotor cortex. In such individuals, rhythms from less affected frontal or parietal cortex (Hudson et al., 1993; Sasaki and Iwata, 2000) may prove better for BCI application. Because these rhythms are recorded from scalp locations closer to facial or temporal muscles, their recording is particularly susceptible to EMG contamination. Unrecognized EMG contamination can mimic actual EEG control and thereby mislead and otherwise impede research aimed at improving these BCI systems. Thus, continued productive development and eventual practical application of these systems to the needs of those with severe motor disabilities require the ability to recognize and eliminate EMG contamination in real-time during online operation.

In theory, a variety of methods might be used to reduce or eliminate EMG contamination. These include relatively simple methods such as linear or non-linear low-pass filtering (Barlow, 1986; Ives and Schomer, 1988; Panych et al., 1989; Sadasivan and Dutt, 1995; Klass, 1995) or rejection of EEG segments that exceed a predefined amplitude threshold (Brunner et al., 1996; Anderer et al., 1999; Junghofer et al., 2000) and more sophisticated methods such as factor decomposition using principal component (Lagerlund et al., 1997) or independent component analysis (Jung et al., 2000). Successful application of any of these methods requires detailed knowledge of the spectral and topographical patterns of cranial EMG contamination. This information is not available at present.

It is known that EMG of skeletal muscles recorded from the skin has a broad frequency distribution from 0 to >200 Hz with several more or less distinct spectral components (Farmer et al., 1993; McAuley et al., 1997; Halliday et al., 1998; Hari and Salenius, 1999; Marsden et al., 1999; Mima and Hallett, 1999; Brown, 2000). These include a 0–5 Hz component thought to reflect a common drive to the motor units, a 10 Hz component thought to reflect motor unit firing and physiological tremor, a 20–30 Hz component (the so-called EMG beta rhythm), and a 35–60 Hz component (the Piper rhythm). EMG from facial muscles also shows a broad frequency distribution from 0 Hz up, with two peaks corresponding to the EMG beta and Piper rhythms (Van Boxtel et al., 1983, 1984; Van Boxtel, 2001).

Current understanding of EMG distribution over the scalp is largely qualitative rather than quantitative. Studies to date have been limited to a few electrode locations, have included data from only a few subjects, have not controlled the strength of muscle contraction, and/or have not included statistical analyses (O'Donnell et al., 1974; Lee and Buchsbaum, 1987; Friedman and Thayer, 1991; Willis et al., 1993). It is known that EMG activity affects alpha, beta, and even delta frequency bands (Barlow, 1986; Klass, 1995; Brunner et al., 1996). However, most automated methods for EMG artifact detection and elimination incorporate the assumption that EMG recorded from the scalp has a broad spectral distribution that begins at 15–20 Hz, and thus can obscure only higher frequency EEG activity (Gotman et al., 1975; Chiappa, 1986; Lee and Buchsbaum, 1987; Sadasivan and Dutt, 1995).

The purpose of the present study was to facilitate the continued development of BCI technology by obtaining from a representative group of adults a detailed quantitative description of the spectral and topographical distributions over the scalp of EMG from frontalis and temporalis muscles. We focused on these two muscles because they are the most common sources of EMG over frontal and central head regions (Barlow, 1986; Klass, 1995). Since the detection and elimination of EMG contamination must ultimately be achieved in each individual BCI user, the goal was to describe both the average results from the entire group of subjects and the range of variation across individuals.

2. Methods

2.1. Subjects

Data were collected from 25 healthy adults, 13 women and 12 men (16–53 years, mean 35). None had a history of a neurological or psychiatric disorder and none was on chronic medication. Most had previously participated in BCI studies and were familiar with the experimental environment. The study was approved by the New York State Department of Health Institutional Review Board and informed consent was obtained from all participants. Lateralization of psychomotor functions was estimated from self-evaluation of handedness, from hand, foot, and eye dominance scores (Bragina and Dobrohotova, 1981), and from the verbal/manual dual task for speech lateralization (Cohen, 1982). The group included 23 left-hemisphere dominant people (lateralization index +26.6–+100%), one right-hemisphere dominant person (−78.57%), and one ambidextrous person (+6.25%).

Ten of the subjects (3 women and 7 men) participated in a study of EMG contamination as a function of strength of frontalis muscle contraction (Experiment 1). All 25 subjects participated in a study of the spectral and topographical distributions of weak (15% maximum) contractions of the frontalis and temporalis muscles (Experiment 2).

2.2. Procedure

EEG and EMG signals were recorded at rest with eyes open (i.e. "relaxation") and during maximum and defined sub-maximum isometric contractions of the frontalis muscles (produced by raising eyebrows) or the temporalis muscles (produced by jaw clenching).

The subject sat in a reclining chair 1.5 m away from a video screen (38 × 28 cm). As described below, the screen

presented visual feedback indicating EMG amplitude so that the subject could maintain a defined level of muscle contraction. Since low-level cranial EMG activity is often present during relaxation (Jensen and Fuglsang-Frederiksen, 1994), the required levels of muscle contraction for each person were defined in terms of that person's range from relaxation to maximum contraction (see below).

As shown in Fig. 1, the screen displayed a cursor and a central target box. The cursor moved vertically (10 steps per second) along the midline of the screen as a function of the sum of the EMG amplitudes for the two homologous muscles (i.e. right and left frontalis or right and left temporalis). To measure the level of muscle contraction, amplitude (square root of power) was calculated with an autoregressive model of order 10 (McFarland et al., 1997a) for the frequency range 17.5–82.5 Hz. The vertical position of the cursor relative to the center of the target box was defined by the difference between the current EMG value and a target value. This target value was either EMG value during relaxation, EMG value during maximum voluntary contraction, or EMG value during a sub-maximum voluntary contraction of 15, 30, or 70% (e.g. the 15% value was the value during relaxation plus 15% of the difference between the value during maximum voluntary contraction and the value during relaxation). Thus, when the EMG value matched the target value, the cursor was in the center of the target box. The sensitivity (i.e. gain) of cursor location was set so that the cursor was at the top or bottom edge of the box when the EMG value was 20% above or below the target value (e.g. the permissible range of EMG amplitude during the sub-maximum contractions was 15 ± 3, 30 ± 6, and 70 ± 14% of maximum, respectively). The subject's goal was to keep the cursor in the box for a required cursor-position maintenance period, which was either 2 or 3 s. He/she was asked to remain motionless during each trial and to try not to blink during the 2 or 3 s cursor-position maintenance period.

An experiment comprised 9–12 2 or 3 min runs. A run comprised 14–17 trials separated by 3 s inter-trial intervals. Fig. 1 shows the sequence of events during a single trial. In each run, frontalis or temporalis muscle contraction controlled cursor position and the required contraction level was: relaxation, 15% maximum, 30% maximum, 70% maximum, or maximum voluntary contraction.

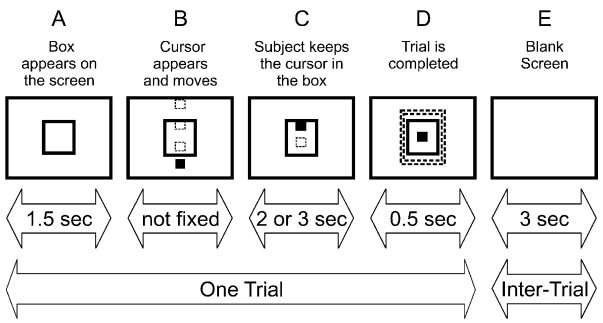

Fig. 1. Sequence of events in a trial. (A) A 7 × 9 cm box (6% of the screen area) appears on the screen. (B) The cursor (1.7 × 1.5 cm, 0.24% of the screen area) appears on the screen and moves vertically controlled by the subject's EMG. (C) The subject maintains the cursor position within the box by appropriate muscle contraction (for 2 s in Experiment 1 or 3 s in Experiment 2). (D) Flashing box signals to the subject that the trial is completed. (E) Inter-trial interval.

Experiment 1 focused on frontalis contraction and consisted of 2–3 relaxation runs, one maximum contraction run, and 2–3 runs each for 15, 30, and 70% contractions. Each run lasted 2 min and comprised 14–17 trials. In each trial, the required cursor-position maintenance period (Fig. 1C) was 2 s.

Experiment 2 included frontalis and temporalis contractions. It consisted of 3 relaxation runs, one maximum frontalis contraction run, one maximum temporalis contraction run, 3 15% frontalis contraction runs, and 3 15% temporalis contraction runs. Each run included 16 trials and lasted 2–3 min. In each trial, the required cursor-position maintenance period (Fig. 1C) was 3 s.

2.3. Data collection and processing

As shown in Fig. 2, EEG was recorded from 64 standard locations (American EEG Society, 1994) referred to the right earlobe using an electrode cap (Electro-cap International), and 4 bipolar EMG signals (right and left frontalis and anterior temporalis muscles) were recorded with 11 mm/2 mm Ag/AgCl cup electrodes.

In Experiment 1, 31 EEG channels from the anterior half of the scalp (i.e. as far back as the coronal line T7–Cz–T8) and the 4 EMG channels were bandpass filtered (0.1–200 Hz, fourth-order Butterworth, down 3% at 180 Hz), amplified (20,000 ×), and digitized at 512 Hz. In Experiment 2, all 64 EEG channels and the 4 EMG channels were filtered (0.1–100 Hz), amplified, and digitized at 256 Hz. The data collected during the 2 or 3 s cursor-position maintenance periods were inspected and the occasional portions displaying prominent non-EMG artifacts (e.g. eyeblink artifacts) were eliminated from further analysis. Horizontal eye movements were rare because the cursor only moved vertically. Vertical eye movements usually did not exceed the 3.5 angular degrees that separated the top and bottom edges of the screen. In Experiment 1, the periods of data analyzed for each subject averaged 58.9 s for relaxation, 49.1 s for 15%, 52.4 s for 30%, and 52.8 s for 70% contraction. In Experiment 2, they averaged 153.6 s for relaxation, 128.9 s for 15% frontalis contraction, and 126.0 s for 15% temporalis contraction.

The digitized EEG data were analyzed with 3 different montages: a standard monopolar montage (i.e. all electrodes referred to the right earlobe), a common average reference (CAR) montage, and a next-nearest neighbor Laplacian montage (McFarland et al., 1997b). The latter two montages were used because of their value for BCIs based on sensorimotor rhythms (McFarland et al., 1997b). For the data from each person provided by each montage under each

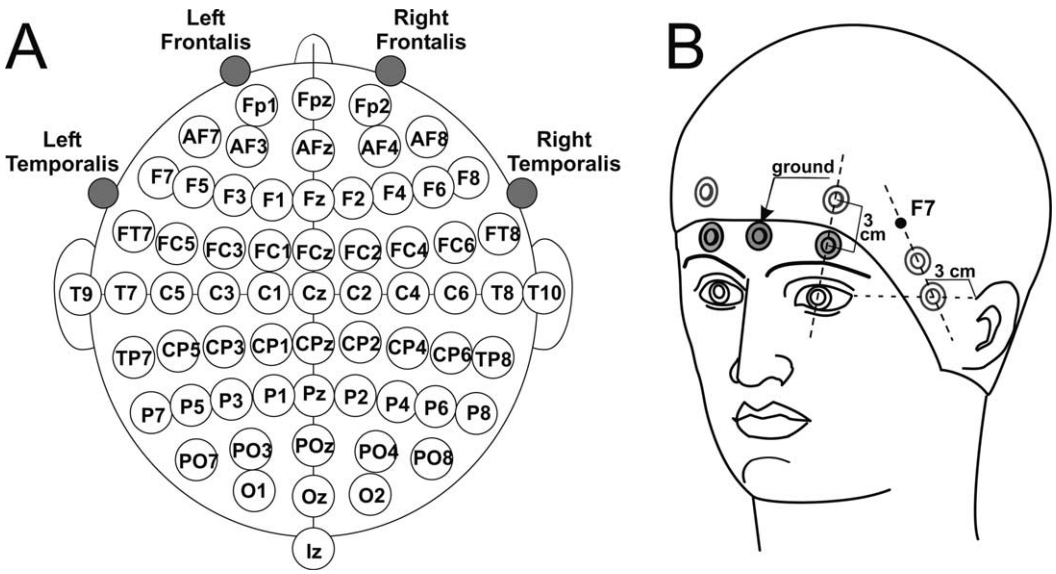

Fig. 2. Scalp electrode positions (A) (according to American EEG Society, 1994) and frontalis and temporalis muscle electrode positions (B). (A) also shows the positions of the 4 muscle electrode pairs (hatched). In (B) frontalis muscle electrodes are positioned on the forehead following Van Boxtel et al. (1983, 1984). Temporalis muscle electrodes are positioned as in previous studies (O'Dwyer et al., 1981; Van Boxtel et al., 1983; Cecere et al., 1996), except that the F7 and F8 scalp locations are used as landmarks instead of the hairline (which was not clear in every subject).

experimental condition, frequency spectra (1 Hz resolution) for each trial were obtained by Fast Fourier Transform and averaged across trials. The effects of muscle contractions were estimated by R^2 (i.e. the proportion of the variance attributable to contraction level) (Wonnacott and Wonnacott, 1977), calculated with the number of observations equal to the number of trials (Wolpaw et al., 2002). Average results for all subjects were calculated with the number of observations equal to the number of subjects (i.e. 25).

For each montage and each contraction level, scalp topographies of the voltage and R^2 values for specific frequency bins were computed by linear interpolation. The scale for the R^2 topographies was set so that the lowest color level (i.e. dark blue) was significant with $P = 0.01$ and the highest (i.e. red) was significant with $P = 0.00001$.

3. Results

3.1. Spectral distribution as a function of muscle contraction level

Fig. 3 presents average (i.e. all 10 subjects of Experiment 1) amplitude spectra for signals recorded from the 4 facial locations and from the anterior half of the scalp during relaxation and during 4 levels of frontalis muscle contraction. The spectra are calculated from the data as they were recorded: bipolar for EMG, and monopolar referenced to the right earlobe for EEG.

As expected, spectral amplitudes are higher at stronger contraction levels, and this increase is most prominent at anterior facial and scalp locations. Strong contractions (maximum and 70%) affect all frequencies from 0 to 200 Hz at all locations. Weak and moderate contractions (15 and 30%) affect frequencies from 5–10 to 200 Hz at the facial and anterior scalp locations and from 15–20 to 200 Hz at central scalp locations.

The shapes of the spectra are similar for facial and anterior frontal scalp locations, even though the signals were referenced differently. The spectra for all contraction levels peak at about 30 Hz and then decline steadily as frequency rises, except for a smaller peak at 45–70 Hz with stronger contractions. The peak frequency increases with contraction level, from 20–25 to 35–38 Hz.

At temporal locations (T7 and T8), the spectra show a broad elevation from 45 to 120 Hz. At central locations, the spectra for strong contractions peak at about 30 Hz, while those for weak contractions show only a modest broad elevation above 15–20 Hz.

In general, the spectra shown in Fig. 3 peak below 40 Hz, decline markedly by 90–100 Hz, and continue to decline smoothly thereafter. Thus, while these data were recorded with a 200 Hz low-pass filter and a sampling rate of 512 Hz, the main features of EMG contamination should be evident with a 100 Hz low-pass filter and a sampling rate of 256 Hz. As described in the next subsections, Experiment 2 used these parameters to record from a larger set of electrodes and thereby delineate EMG contamination over the entire scalp.

3.2. Spectral distribution as a function of the active muscle

3.2.1. Average data

Fig. 4 presents average (i.e. all 25 subjects of Experiment 2) spectral data from facial and scalp locations during

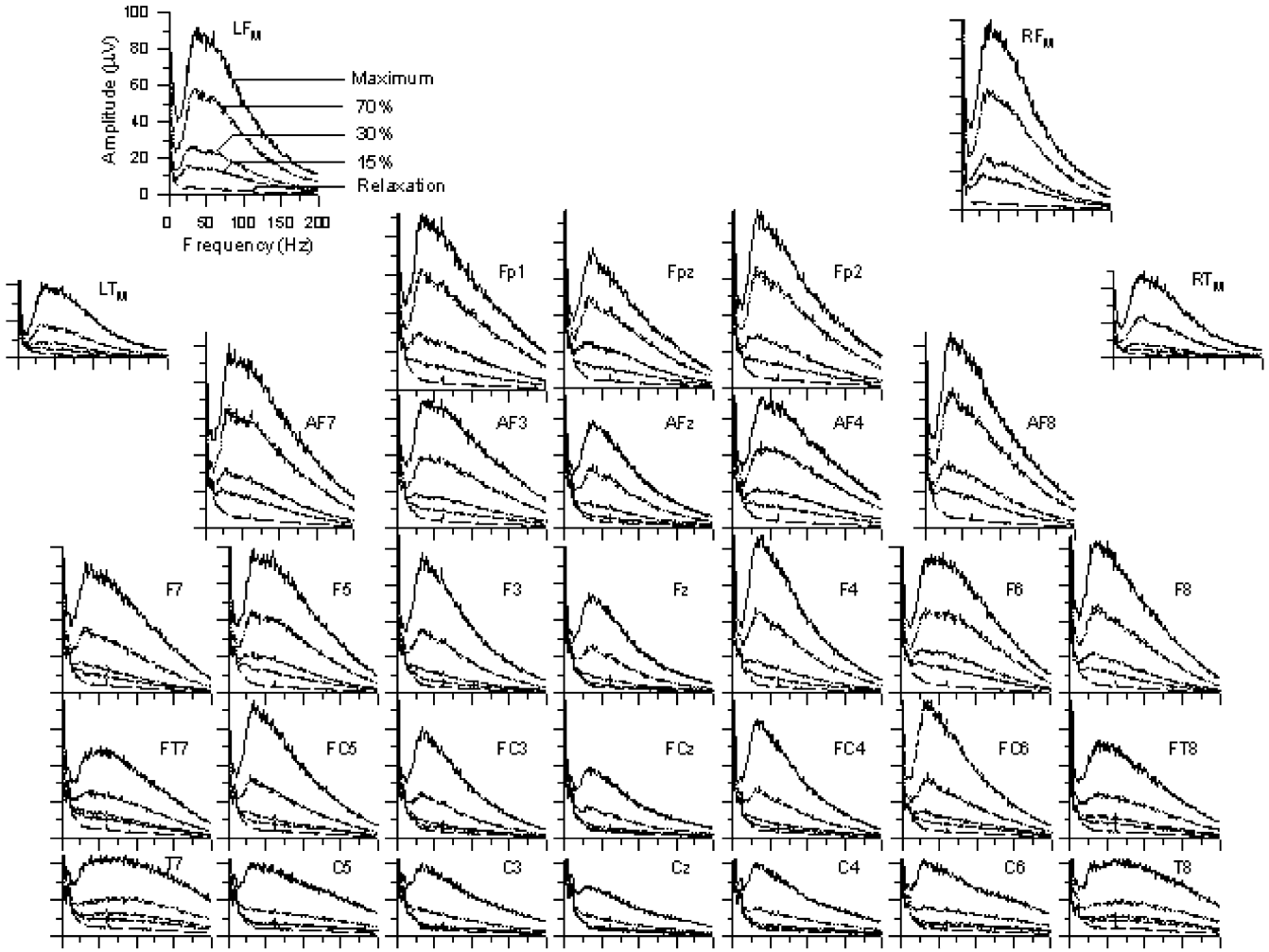

Fig. 3. Average amplitude spectra for 10 subjects of signals recorded from the 4 facial locations (over frontalis muscles, LF_M and RF_M, and temporalis muscles, LT_M and RT_M) and from the frontal half of the scalp (electrode locations as in Fig. 2) during relaxation and during 4 levels of frontalis muscle contraction (15, 30, 70, and 100% of maximum). The signals were sampled at 512 Hz and bandpass filtered at 0.1–200 Hz. All spectra are plotted on the scale shown at the top left. (In some spectra, a small narrow 60 Hz artifact reflecting power line frequency is evident.)

relaxation and weak (15% maximum) contraction of the frontalis or temporalis muscles. To avoid any possibility of reference-related hemispheric asymmetry, the data were re-referenced to a CAR prior to spectral analysis.

Both frontalis and temporalis muscle contractions increase spectral amplitude at all locations. Increase is most prominent at peripheral locations over or near the contracting muscle: anterior locations for frontalis contraction, and lateral frontal and temporal locations for temporalis contraction. It is particularly relevant for BCI research that the temporalis contraction also produces substantial amplitude increases over sensorimotor cortices (e.g. C3 and C4). In addition, substantial increase occurs in the temporal area during frontalis contraction and in the frontal area during temporalis contraction. This effect probably reflects co-contraction of the two groups of muscles.

As expected for CAR spectra during relaxation, all scalp locations show a peak in the alpha frequency range (about 10 Hz) that is largest in the parieto-occipital area. In this area, the peak decreases during frontalis or temporalis contraction. The decrease presumably reflects contraction-related attenuation of mu rhythms and also visual alpha rhythms (suggesting that maintenance of cursor position requires more attention in the contraction condition than in the relaxation condition) (Niedermeyer, 1999). In contrast, during temporalis contraction, the peak increases in temporal areas. This suggests that temporalis EMG activity has a frequency component in the alpha range. During either frontalis or temporalis contraction, the parieto-occipital spectral amplitudes at 15–23 Hz decrease, probably reflecting contraction-related attenuation of EEG beta activity.

While all spectra show broad-banded EMG contamination, their shapes differ with location and active muscle. For frontalis contraction, the frontal and frontocentral spectra peak at 20–30 Hz and the peak frequency is highest at the most anterior locations. For temporalis contraction, spectra at temporal and nearby locations are broadly elevated with the maximum at 40–80 Hz and a smaller

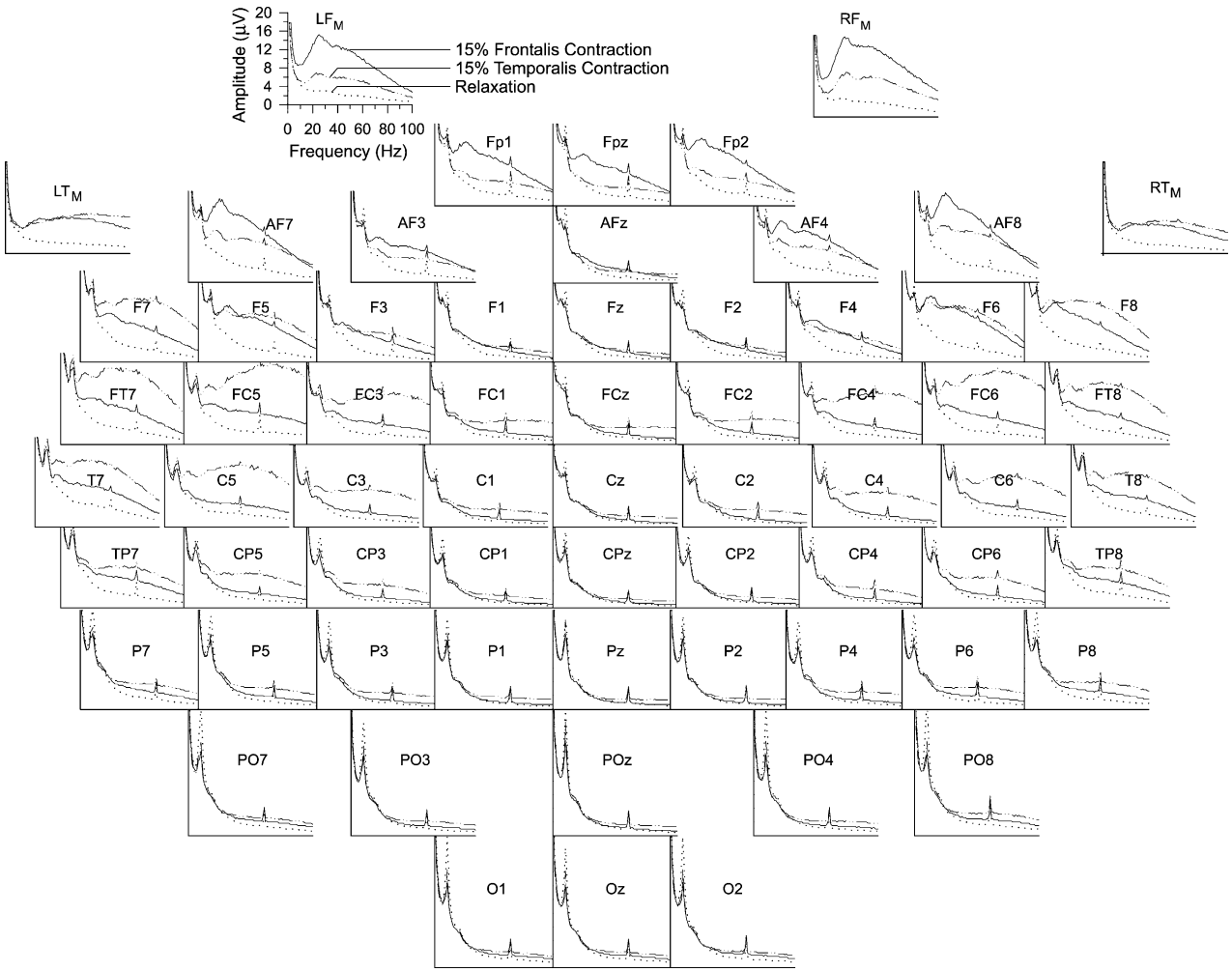

Fig. 4. Amplitude spectra of the signals from facial and scalp locations (Fig. 2) during relaxation and during weak (15% maximum) contraction of frontalis or temporalis muscles. The signals were sampled at 256 Hz, bandpass filtered at 0.1–100 Hz, re-referenced to a CAR, and averaged across 25 subjects. (As in Fig. 3, a 60 Hz artifact reflecting power line frequency is evident.)

elevation at about 20 Hz. At midcentral and posterior locations, only small broad-banded elevation is seen.

EMG contamination is greatest at frontal locations for frontalis contraction, and at temporal and nearby locations for temporalis contraction. All contraction-related peaks in the beta and gamma frequency ranges attenuate and broaden from peripheral frontal and temporal locations toward central and posterior locations. Even weak contraction of frontalis or temporalis muscles affects spectra across a broad frequency range that includes EEG frequency bands. As Fig. 4 indicates, the lowest frequencies affected by muscle activity range from 0 to 25 Hz depending on scalp location. This important issue is evaluated in more detail in Section 3.3 with statistical methods.

3.2.2. Individual data

The spectra for individual subjects frequently displayed much sharper spectral peaks than those evident in the average data of Figs. 3 and 4. Fig. 5 (right side) presents amplitude spectra (Laplacian reference) from selected locations for 3 individuals.

All 3 people show sharp peaks in the beta frequency range. Similarly, sharp beta peaks were seen in nearly every individual. The broad peaks in the average spectra of Figs. 3 and 4 presumably reflect inter-subject differences in peak frequency. Such differences are evident in Fig. 5. We assessed the range of inter-subject variation in the frequency of these EMG spectral peaks using the spectra from facial locations to avoid any possible confusion with EEG beta activity. For frontalis muscle contraction, the peak frequency varied from 16 to 38 Hz, with 65% in the range 22–27 Hz. For temporalis muscle contraction, the peak frequency varied from 13 to 34 Hz, with 69% in the range 19–24 Hz. The prominence and sharpness of these beta frequency peaks, both at facial locations and more posteriorly as well (e.g. Fig. 5), suggests that such EMG activity could easily be misinterpreted as EEG activity.

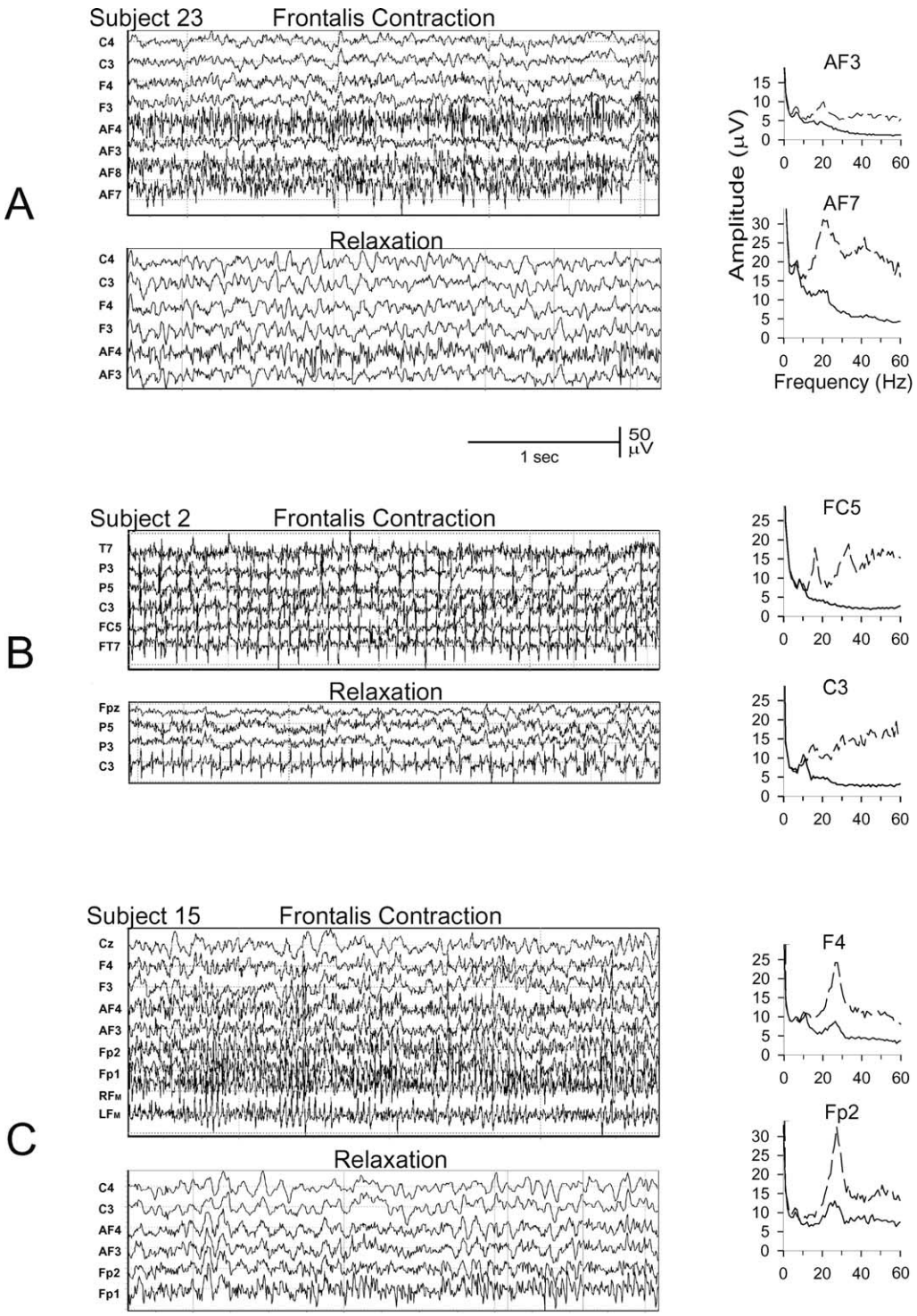

Fig. 5. Examples of the 3 distinct visual patterns of EMG contamination with sample spectra (solid line, relaxation; dashed line, 15% frontalis contraction). (A) Common "noise-like" pattern. (B) "Railroad cross-tie" pattern. (C) Beta rhythm-like pattern.

3.3. Topographical distribution of the effects of muscle contraction

Fig. 6 presents the R^2 topographies for the significant effects of frontalis and temporalis muscle contractions. Topographies are shown for 4 Hz bins spanning the 0–40 Hz range and for representative higher-frequency bins up to 100 Hz. Data for monopolar, CAR, and Laplacian montages are shown to compare the sensitivities of the different spatial filters to EMG contamination.

For both muscles and with all 3 spatial filters, the EMG activity evident in Fig. 6 has two major features. First, it is

present at the lowest frequency range (2 and 6 Hz bins), increases with frequency, and at higher frequencies involves the entire scalp. Secondly, it is greatest at peripheral locations near or over the active muscle (i.e. frontal for frontalis contraction, temporal for temporalis contraction). The spectral data of Fig. 4 confirm that these effects represent EMG activity spreading over the scalp.

Contraction of either muscle has an additional more modest effect, evident at 8–24 Hz in posterior regions for both muscles and at 8–16 Hz in the central region for frontalis. As Fig. 4 indicates, this effect is a decrease in activity. It presumably reflects contraction-related attenuation of EEG components. This attenuation is most prominent in the alpha frequency band. In other scalp locations, contraction-related EEG attenuation is probably obscured by the greater increases in EMG activity. The effects of both frontalis and temporalis contractions are largely symmetrical in these average results (though some individuals showed asymmetrical effects, see Section 3.5).

While the pictures shown by the 3 spatial filters are similar, they do differ to some extent. In the theta frequency range (6 Hz bin), EMG effects are evident only for the Laplacian montage. At the lowest frequencies (2 Hz bin) and in the alpha range (10 Hz bin), effects are evident for all 3 montages, but they are most widely distributed for the Laplacian and least so for the monopolar. On the other hand, as frequency increases, EMG effect comes to involve the entire scalp first for the monopolar montage (i.e. by the 38 Hz bin for frontalis and the 22 Hz bin for temporalis) and last for the Laplacian montage (i.e. by the 98 Hz bin for frontalis and the 38 Hz bin for temporalis).

3.4. Visual appearance of EMG contamination

Visual examination of individual records identified 3 distinct patterns of EMG contamination. Fig. 5 illustrates

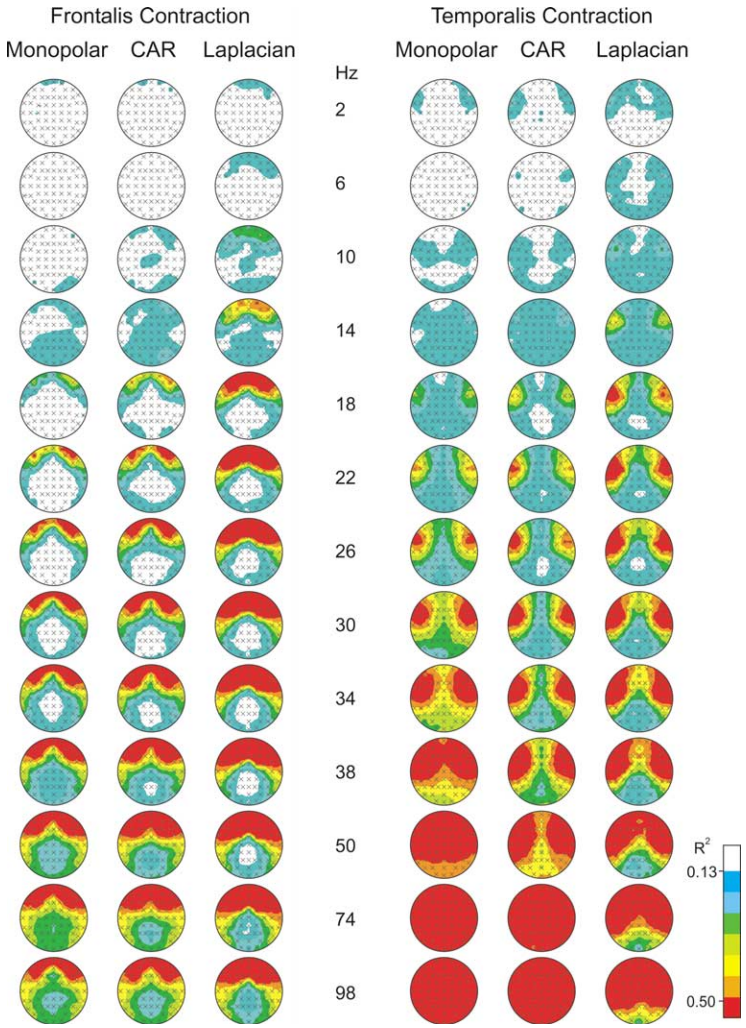

Fig. 6. Average R^2 topographic maps (nose at top; 64 channels as in Fig. 2A) for all 25 subjects for monopolar, CAR, and Laplacian montages for 4 Hz bins for 15% frontalis contraction vs. relaxation (left) and 15% temporalis contraction vs. relaxation (right). Each 4 Hz bin is labeled with its center frequency. The R^2 scale is limited to significant effects: the lowest (i.e. dark blue) values are significant at $P < 0.01$ and the highest (i.e. red) are significant at $P < 0.00001$.

these patterns with representative segments of the raw (i.e. monopolar) data.

3.4.1. Common "noise-like" pattern

The first pattern of EMG contamination occurred at one or more locations in every person during contraction and often during relaxation as well. It comprises irregular spikes and waveforms of varying frequency. It may be high in amplitude and largely obscure EEG signals (e.g. Fig. 5A, frontalis contraction: AF4, AF7, AF8) or low in amplitude (Fig. 5A, frontalis contraction: F4, F3, AF3; relaxation: AF4). With spectral analysis (Fig. 5A, AF3 and AF7 spectra), this form of EMG contamination may show quite sharp peaks around 20 Hz. During relaxation, it was most often present at the periphery, but it could be anywhere except for centro-parietal locations.

3.4.2. "Railroad cross-tie" pattern

The second pattern, previously described as a railroad cross-tie pattern (Barlow, 1986), was present in 20 of the 25 subjects at one or more locations during contraction and/or during relaxation. It consists of persistent rhythmical spikes at a rate of 8–18 per second that may greatly exceed EEG activity in amplitude (e.g. Fig. 5B, frontalis contraction: P3, P5, C3, FC5, FT7; relaxation: C3). The spectra typically show one or two peaks in the beta range. For the subject in Fig. 5B, these peaks are at 15 Hz at C3, and at 15 and 32 Hz at FC5.

Fig. 7A shows for each scalp location and each condition the number of subjects among the population of 25 who displayed this pattern.

During relaxation, 12 of 25 subjects showed this pattern at a single usually lateral location, most often T7. During frontalis or temporalis muscle contraction, the pattern was more common. While it could occur at essentially any scalp location except those along the midline, it tended to be more posterior during frontalis contraction than during temporalis contraction. It was present less often over the active muscles than over the surrounding areas. Over all subjects, it was equally common on right and left sides, but was typically unilateral in each one.

Many subjects displayed the noise-like pattern and the railroad cross-tie pattern simultaneously at different locations. For example, the top panel in Fig. 5B shows the first pattern at T7 and the second pattern at the other locations.

3.4.3. Beta rhythm-like pattern

The third pattern, found in 6 of the 25 subjects, is illustrated in Fig. 5C. It is composed of waves rather than spikes and resembles an EEG beta rhythm, though it differs from typical EEG beta in the sharp shape of the waves (e.g. Fig. 5C, frontalis contraction: F4, F3, AF4, AF3, Fp2, Fp1, and facial locations RF_M and LF_M; relaxation: Fp1 (middle and right parts of trace)). During muscle contraction, it often appeared in spindles (e.g. Fig. 5C, frontalis contraction: Fp2, Fp1, and facial locations (left part of traces)). Recognition of this form of EMG contamination may be difficult in individuals who also have a prominent EEG beta rhythm (e.g. Fig. 5C, frontalis contraction: Cz). However, the EMG beta may be recognized by its topography; it was largest at the most anterior locations. For example, in the spectra of Fig. 5C, the sharp peak at 26 Hz is higher at Fp2 than at F4 for both relaxation (solid lines) and contraction (dashed lines).

Fig. 7B shows for each scalp location and each condition the number of subjects among the population of 25 who displayed this pattern. During relaxation, it was found only at the most anterior locations. During frontalis contraction, it was most common anteriorly. During temporalis contraction, it was again most prominent anteriorly, but could extend over essentially the entire scalp. In all cases, its myogenic origin was indicated by the fact that its amplitude was greatest at the most anterior scalp locations and at facial locations.

3.5. Individual differences in topographical distribution of EMG contamination

Fig. 8 shows scalp topographies (with the Laplacian spatial filter) for 2 Hz bins from 1 to 91 Hz for individual subjects during frontalis or temporalis contraction. These examples have been chosen to reflect the full range of results across the 25 subjects.

In all the subjects, the effects of muscle contractions increased in strength and expanded across the scalp as frequency increased. In comparison to the average topographies of Fig. 6, the individual topographies in Fig. 8 are sharper, with more prominent high (i.e. red) values and low (i.e. white) values and less prominent intermediate values. This presumably reflects the absence of the smoothing produced by averaging all the subjects (e.g. Fig. 6).

As illustrated in Fig. 8, muscle contraction effects were much greater and more widespread in some people (e.g. #6 for frontalis contraction, #5 and #8 for temporalis contraction) than in others. They were asymmetrical in a few subjects for frontalis contraction (e.g. #5) and in more with temporalis contraction (e.g. #5, #8, #11). Among the 25 subjects, the effects of temporalis contraction were symmetrical in 10, stronger on the left in 8, and stronger on the right in 7. Individuals also differed in the location of the strongest effect. For frontalis contraction, the greatest effect was usually at the anterior edge of the scalp (e.g. #5, #19). However, in some individuals, EMG contamination in the alpha frequency range was focused elsewhere (e.g. at F5, FC3, and FC5 in #6, and at AF4 in #10). The myogenic origin of these effects was confirmed by their increases in spectral amplitude during contraction. For temporalis contraction, the effects were usually focused near the muscles, but could be focused more centrally (e.g. effects in the alpha range at frontocentral locations in #5, #8, and #22). This shift from the periphery was probably not

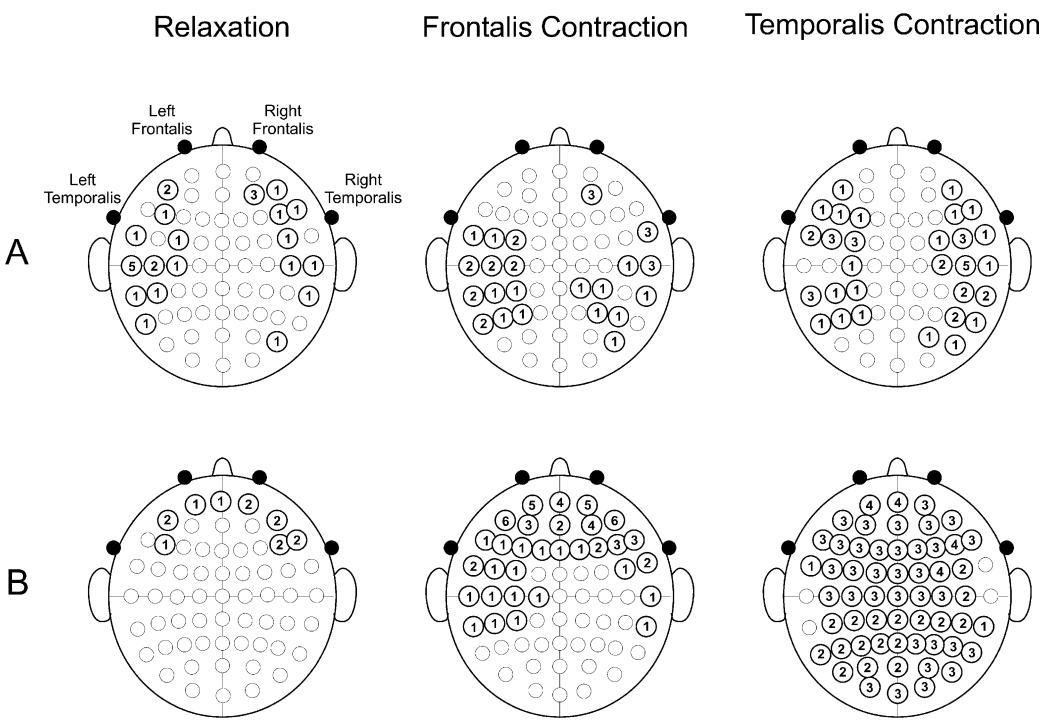

Fig. 7. Scalp distributions of "railroad cross-tie" (A) and beta rhythm-like (B) patterns of EMG contamination during relaxation, frontalis contraction, and temporalis contraction. At each location, the number of subjects (from the population of 25) who displayed the pattern is shown.

attributable to the Laplacian montage since it was found with the monopolar and CAR montages as well. (Furthermore, the average topographies in Fig. 6 are similar for the 3 montages.)

The examples presented in Fig. 8 illustrate the considerable inter-individual variation in the topography of EMG contamination. Because EMG contamination has no single characteristic topography, considerable care

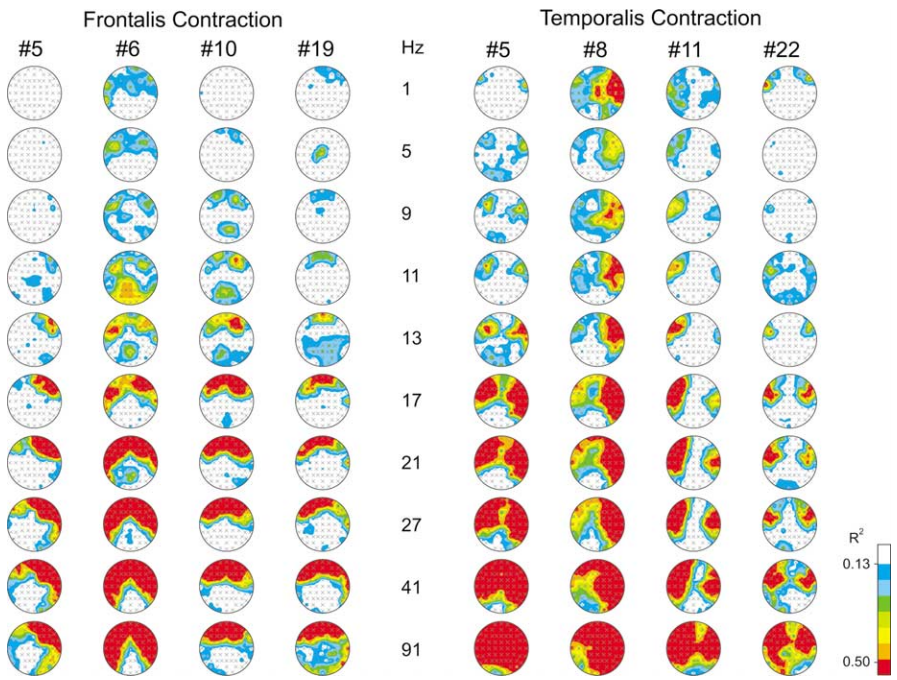

Fig. 8. Representative individual subject data for 15% frontalis and temporalis muscle contractions. R^2 values are calculated in 2 Hz bins (each labeled with its center frequency) for the Laplacian spatial filter. Each column displays data from one subject (subject number at top of column). As in Fig. 6, the R^2 scale is limited to significant effects: the lowest (i.e. dark blue) values are significant at $P < 0.01$ and the highest (i.e. red) are significant at $P < 0.00001$.

may be needed to recognize such contamination in an individual.

4. Discussion

This study set out to describe the amplitude and spectral content of EMG from frontalis and temporalis muscles recorded from a comprehensive set of scalp locations. Its central purpose was to provide basic knowledge needed for the evaluation of EMG artifacts during the operation of EEG-based BCI systems and essential for the design of methods for detecting these artifacts online and minimizing their impact.

4.1. Main features of EMG activity near the active muscle

With frontalis or temporalis muscle contraction, the signals recorded over or near the muscles show energy at all frequencies from 0 to 200 Hz. Spectra for frontalis contraction show a main peak at about 30 Hz, a smooth elevation from 45 to 60 Hz, and a progressive decrease thereafter. Spectra for temporalis contraction show the highest amplitude from 35 to 80 Hz and a small peak at about 20 Hz. The shape of the spectra and the tendency for peak frequency to increase with contraction strength were comparable for the bipolar recordings from facial locations and the monopolar recordings from peripheral scalp locations.

The results are consistent with previous descriptions of the surface EMG of skeletal muscle in showing the EMG beta and Piper (35–60 Hz) rhythms (Farmer et al., 1993; Gibbs et al., 1995; McAuley et al., 1997; Halliday et al., 1998; Hari and Salenius, 1999; Marsden et al., 1999; Mima and Hallett, 1999; Brown, 2000). They also agree with previous descriptions of frontalis and temporalis EMG recorded directly over the muscles (Van Boxtel et al., 1983, 1984). The apparently linear increase in spectral amplitudes as contraction strength increases fits previous observations of the masticatory muscles (Scholle et al., 1992). Furthermore, the observation that the frequency of the main spectral peak increases with contraction strength is consistent with the finding of Conwit et al. (1999) in the quadriceps femoris during isometric contractions at fixed force levels.

The close spectral similarity evident in Figs. 3 and 4 between the signals recorded directly from the cranial muscles and the signals recorded from nearby peripheral scalp electrodes of the 64-channel montage suggests that during even modest muscle contractions these scalp electrodes record mostly EMG rather than EEG activity.

4.2. Spread of EMG activity over the scalp

In general, while EMG amplitude was greatest near the active muscles, even relatively weak (15%) contraction of frontalis or temporalis muscles produced EMG activity detectable over the entire scalp. The shape of the spectra differed with scalp location.

For frontalis contraction, the spectra for the medial frontocentral area showed a broad elevation from 20 to 100 Hz, rather than the clear peak at about 30 Hz seen over the muscles. Similarly, for temporalis contraction, the spectra flattened with distance from the muscles, presumably reflecting greater attenuation of the lower-frequency EMG activity responsible for the spectral peak than of the higher-frequency EMG. This finding is consistent with evidence that spread by volume conduction is greater for higher frequencies (Srinivasan and Dutt, 1998).

The results indicate that an assumption often incorporated into EMG artifact elimination methods – that EMG contamination is the same from about 20 to above 100 Hz (Gotman et al., 1975; Chiappa, 1986; Lee and Buchsbaum, 1987; Sadasivan and Dutt, 1995) – is not correct for most scalp areas. In fact, the frequency dependence of EMG contamination varies with the active muscle and the recording location.

4.3. Effectiveness of different spatial filters in revealing EMG contamination

The 3 spatial filters created by the monopolar, CAR, and Laplacian electrode montages all showed that the topographical extent of the effects of muscle contraction grows as frequency rises, and is greatest above 40 Hz. The 3 filters were also similar in showing that EMG contamination began at 0 Hz near the contracting muscles. At the same time, they differed in some respects. The monopolar filter detected temporalis EMG activity near the contracting muscles in the delta and alpha ranges, but not in the theta range. The Laplacian spatial filter showed widespread temporalis and frontalis EMG contamination over all EEG frequencies. The CAR filter gave intermediate results.

Assuming that the EMG signal spreads across the scalp by volume conduction, it might be expected that the Laplacian spatial filter would tend to eliminate it (Nunez, 1990; Srinivasan et al., 1996). This expectation (Akay and Daubenspeck, 1999) is not supported by the present study. Indeed, the opposite results occurred for lower frequencies (i.e. 0–20 Hz). The high sensitivity of the Laplacian spatial filter to EMG contamination is probably due to the fact that the EMG signal reflects activation of multiple muscles and multiple motor units in each muscle and that these sources differ in location, timing, and form.

4.4. EMG contamination in the EEG frequency range

While the fact that EMG contaminates EEG in the beta frequency range (i.e. 14–30 Hz) and above is well-established (Barlow, 1986), the available information concerning the extent to which it contaminates EEG in lower frequency ranges is sparse and contradictory

(O'Donnell et al., 1974; Lee and Buchsbaum, 1987; Friedman and Thayer, 1991; Willis et al., 1993; Brunner et al., 1996). The present study shows that EMG can contaminate all EEG frequency bands and that the contamination differs with scalp location.

In the present study, the delta frequency band (0–4 Hz) was affected at locations near the active muscles: in the anterior frontal area for frontalis contraction and in the temporal area for temporalis contraction. This localization suggests that oculomotor artifacts were not responsible (although electrodermal activity or skin movements that change electrode impedance could conceivably play a role). In surface EMG, the low-frequency 0–5 Hz spectral component is considered to be a true EMG component, reflecting a common drive to motoneurons (Marsden et al., 1999; Brown, 2000).

Brunner et al. (1996) reported that EMG contamination of EEG is minimal in the theta range. In the present study, this depends on the spatial filter. In the monopolar and CAR data EMG contamination was greater in the delta than in the theta range, while in the Laplacian data it was similar across the EEG frequency range.

The present data show that EMG contamination of EEG signals in the alpha frequency range is widespread over the scalp. Frontalis EMG significantly affects the alpha range in the frontal and frontocentral areas, while temporalis EMG affects the alpha range both in lateral scalp areas and more central locations (C3 and C4). In surface EMG of skeletal muscles, two different alpha range components have been described: single motor unit spikes typically firing at 6–15 Hz and physiological tremor (Conway et al., 1995; Hari and Salenius, 1999; Mima and Hallett, 1999; Brown, 2000). While the tremor, prominent in the extremities, does not seem to be evident in facial muscle activity, we did observe at scalp locations rhythmical spikes forming the railroad cross-tie pattern (Barlow, 1986). The topography of this pattern (Fig. 7) suggests that these rhythmical spikes originate in temporal muscles. Often, this pattern was evident in the spectra as increased alpha band activity during muscle contraction as compared to relaxation.

Muscle contraction effects were stronger and more widespread in the beta range than in the alpha range. A previous report (Friedman and Thayer, 1991) noted that EMG had a stronger effect in the alpha range than in the beta range. However, this earlier study did not distinguish actual EMG from EEG attenuation associated with muscle contraction (which is likely to be most marked in the alpha band), and thus cannot be directly compared with the present study.

4.5. EEG changes with muscle contractions

Contraction-related attenuation of EEG components was generally much less prominent than EMG contamination. EEG attenuation was clearly observed only in scalp areas and at frequency ranges that were largely free from EMG activity. Contraction-related enhancement of theta range activity in the medial frontocentral area was apparent in some subjects; and attenuation of alpha range activity was seen at parieto-occipital locations in most subjects. Attenuation was less often evident for the posterior beta activity, probably because in about one-third of subjects the effects of temporalis EMG were evident in the parietal region above 16 Hz. During frontalis contraction, attenuation of EEG mu and beta rhythms in the central scalp area was evident in both the average data and in the data from most individuals. However, such attenuation was not seen during temporalis contraction, probably because it was obscured by spread of temporalis EMG to the central area. These results clearly demonstrate that detection and/or prevention of EMG contamination are important not only for BCI studies focused on rhythms recorded from frontal scalp area but also for those focused on mu and beta rhythms recorded over sensorimotor cortex.

4.6. Intra- and inter-individual differences in EMG contamination

Visual inspection of the signals revealed 3 distinct patterns of EMG contamination. Often two of them were evident at different locations in the same subject. The most frequent pattern, which is generally appreciated as indicative of EMG artifact, looks like high-frequency noise superimposed on EEG activity. The second, the railroad cross-tie pattern, consists of rhythmical EMG spikes superimposed on EEG. The third and least common variant resembles EEG beta activity. The spectra of the first pattern are relatively flat (though they may show prominent elevations); the spectra of the second often show peaks in the alpha and/or low beta range; and the spectra of the third show a sharp peak in the beta range (20–30 Hz).

The topography of EMG contamination, particularly with frontalis contraction, often indicates co-contraction, unilateral or bilateral, of other muscles in addition to the target muscle group (e.g. Fig. 8, subject #6, left temporal area during frontalis contraction, 12 Hz and above). This observation is consistent with previous reports that co-contraction of different facial muscles is common (Clark et al., 1993; Winter et al., 1994; Zafas et al., 1995). Individual variations in co-contraction presumably account for much of the inter-individual variation in the spectral and topographical features of EMG contamination.

The locations of maximum EMG contamination varied markedly across individuals. In two-thirds of the subjects, frontalis EMG contamination was greatest at the most anterior locations, usually Fp1 or AF8. In contrast, temporalis EMG contamination was most often focused not at the edge but at nearby locations, e.g. FC5 or FC6. If the maximum locations are found to remain the same in each individual over time, they might prove particularly

valuable for development of automatic online EMG detection algorithms.

4.7. Detection and elimination of EMG contamination

Ontogenetically, structurally, and functionally facial muscles appear to be a hybrid of somatic and smooth muscles (Sumitsuji, 1986) and typically show tonic activity. As a result, some degree of EMG contamination is probably present in most EEG recordings. Thus, the key issue for an EEG project is to what extent this contamination interferes with its goals. The present study shows that EMG contamination must be considered a potential problem for all BCI studies involving EEG rhythms, particularly, those recorded over frontal areas but also those recorded elsewhere on the scalp. Thus, such studies need to incorporate comprehensive multichannel data collection and data evaluation designed to detect EMG contamination of the EEG signal features used for communication and control by the BCI system.

The detection of EMG contamination requires appropriate spectral and topographical analyses. Evaluation at one or a few locations and in one or a limited number of frequency bands is not adequate. With such limited analysis, EMG contamination may masquerade as EEG activity and lead to erroneous conclusions (e.g. Lauer et al., 1999, 2000). This is particularly important for BCI studies using EEG beta or gamma band activity. A sufficiently comprehensive spectral and topographical evaluation can usually recognize EMG contamination. While EMG beta peaks in the spectra can be sharper and larger than EEG beta peaks, they are typically accompanied by higher frequency activity, including activity above 40 Hz. Even if such higher-frequency activity is not seen in the spectra (as can occur with weak muscle contraction), EMG activity in the EEG frequency bands can usually be recognized by its peripheral location in scalp topographies.

The simplest approach to eliminating the effects of EMG contamination is to use amplitude in an appropriate frequency band(s) at an appropriate peripheral location(s) to measure this contamination and suspend data collection when this amplitude exceeds a defined criterion. While this simple method has proved effective (McFarland et al., 1997a), its value is limited to situations in which EMG contamination occurs infrequently and/or is subject to voluntary control by the subject. When EMG contamination is always or usually present and the subject cannot suppress it, other methods for eliminating it from the recorded signal are essential.

The present data imply that EMG contamination and EEG have substantial statistical independence from each other both temporally and spatially. This suggests that a spatial Independent Components Analysis (ICA) (Jung et al., 2000) could be an effective method for detecting EMG contamination and then removing it from the signals used for BCI communication and control. The implementation of this method might be facilitated by preliminary recording in which the subject voluntarily contracted specific muscles. The accuracy, reliability, and online practicality of this and other possible methods for detecting and eliminating EMG contamination remain to be explored.

Acknowledgements

We are grateful to our subjects for their conscientious participation in the study. We thank Mr. William A. Sarnacki for technical assistance and Dr. Ann M. Tennissen for reviewing the manuscript. This work was supported by grants from the National Center for Medical Rehabilitation Research, NICHD, NIH (HD30146); from NIBIB and NINDS, NIH (EB00856); and from the ALS Hope Foundation.

References

Akay M, Daubenspeck JA. Investigating the contamination of electroencephalograms by facial muscle electromyographic activity using matching pursuit. Brain Lang 1999;66:184–200.

American EEG Society. Guideline thirteen: guidelines for standard electrode position nomenclature. J Clin Neurophysiol 1994;11:111–3.

Anderer P, Roberts S, Schlogl A, Gruber G, Klosch G, Herrmann W, Rappelsberger P, Filz O, Barbanoj MJ, Dorffner G, Saletu B. Artifact processing in computerized analysis of sleep EEG – a review. Neuropsychobiology 1999;40:150–7.

Barlow JS. Artifact processing (rejection and minimization) in EEG data processing. In: Lopes da Silva FH, Storm van Leeuwen W, Remond A, editors. Handbook of electroencephalography and clinical neurophysiology. Revised series, vol. 2. Amsterdam: Elsevier; 1986. p. 15–62.

Bragina NN, Dobrohotova TA. Funkcionalnye asimmetrii cheloveka. (Functional asymmetry of the human) Moscow: Medicina; 1981. [in Russian].

Brown P. Cortical drives to human muscle: the Piper and related rhythms. Prog Neurobiol 2000;60:97–108.

Brunner DP, Vasko RC, Detka CS, Monahan JP, Reynolds CF, Kupfer DJ. Muscle artifacts in the sleep EEG: automated detection and effect on all-night EEG power spectra. Sleep Res 1996;5:155–64.

Cecere F, Ruf S, Pancherz H. Is quantitative electromyography reliable? J Orofac Pain 1996;10:38–47.

Chiappa KH. Progress in topographic mapping of neurophysiological data. In: Duffy FH, editor. Topographic mapping of brain electrical activity. Boston, MA: Butterworths; 1986. p. 393–6.

Clark GT, Browne PA, Nakano M, Yang Q. Co-activation of sternocleidomastoid muscles during maximum clenching. J Dent Res 1993;72:1499–502.

Cohen G. Theoretical interpretations of lateral asymmetries. In: Beamont JG, editor. Divided visual field studies of cerebral organisation. London: Academic Press; 1982.

Conway BA, Farmer SF, Halliday DM, Rosenberg JR. On the relation between motor-unit discharge and physiological tremor. In: Taylor A, Gladden MH, Durbaba R, editors. Alpha and gamma motor systems. New york, NY: Plenum Press; 1995. p. 596–8.

Conwit RA, Stashuk D, Tracy B, McHugh M, Brown WF, Metter EJ. The relationship of motor unit size, firing rate and force. Clin Neurophysiol 1999;110:1270–5.

Farmer SF, Bremner FD, Halliday Rosenberg JR, Stephens JA. The frequency content of common synaptic inputs to motoneurons studies

during voluntary isometric contraction in man. J Physiol 1993;470: 127–55.
Friedman BH, Thayer JF. Facial muscle activity and EEG recordings: redundancy analysis. Electroenceph clin Neurophysiol 1991;79: 358–60.
Gibbs J, Harrison LM, Stephens JA. Organization of inputs to motoneurone pools in man. J Physiol 1995;485(1):245–56.
Gotman J, Gloor P, Ray WF. A quantitative comparison of traditional reading of the EEG and interpretation of computer-extracted features in patients with supratentorial brain lesions. Electroenceph clin Neurophysiol 1975;38:623–39.
Halliday DM, Conway BA, Farmer SF, Rosenberg JR. Using electroencephalography to study functional coupling between cortical activity and electromyograms during voluntary contractions in humans. Neurosci Lett 1998;241:5–8.
Hari R, Salenius S. Rhythmical corticomotor communication. NeuroReport 1999;10:R1–R10.
Hudson AJ, Kiernan JA, Munoz DG, Pringle CE, Brown WF, Ebers GC. Clinicopathological features of primary lateral sclerosis are different from amyotrophic lateral sclerosis. Brain Res Bull 1993; 30:359–64.
Ives JR, Schomer DL. A 6-pole filter for improving the readability of muscle contaminated EEGs. Electroenceph clin Neurophysiol 1988;69: 486–90.
Jensen R, Fuglsang-Frederiksen A. Quantitative surface EMG of pericranial muscles. Relation to age and sex in a general population. Electroenceph clin Neurophysiol 1994;93:175–83.
Jung TP, Makeig S, Humphries C, Lee TW, McKeown MJ, Iragui V, Sejnowski TJ. Removing electroencephalographic artifacts by blind source separation. Psychophysiology 2000;37:163–78.
Junghofer M, Elbert T, Tucker DM, Rockstroh B. Statistical control of artifacts in dense array. Psychophysiology 2000;37:523–32.
Klass DW. The continuing challenge of artifacts in the EEG. Am J EEG Technol 1995;35:239–69.
Kostov A, Polak M. Parallel man-machine training in development of EEG-based cursor control. IEEE Trans Rehabil Eng 2000;8:203–5.
Lagerlund TD, Sharbrough FW, Busacker NE. Spatial filtering of multichannel electroencephalographic recordings through principal component analysis by singular value decomposition. J Clin Neurophysiol 1997;14:73–82.
Lauer RT, Peckham PH, Kilgore KL. EEG-based control of a hand grasp neuroprosthesis. NeuroReport 1999;10:1767–71.
Lauer RT, Peckham PH, Kilgore KL, Heetderks WJ. Applications of cortical signals to neuroprosthetic control: a critical review. IEEE Trans Rehabil Eng 2000;8:205–8.
Lee S, Buchsbaum MS. Topographic mapping of EEG artifacts. Clin Electroencephalogr 1987;18:61–7.
Marsden JF, Farmer SF, Halliday DM, Rosenberg JR, Brown P. The unilateral and bilateral control of motor unit pairs in the first dorsal interosseous and paraspinal muscles in man. J Physiol 1999;521: 553–64.
McAuley JH, Rothwell JC, Marsden CD. Frequency peaks of tremor, muscle vibration and electromyographic activity at 10 Hz, 20 Hz and 40 Hz during human finger muscle contraction may reflect rhythmicities of central neural firing. Exp Brain Res 1997;114: 525–41.
McFarland DJ, Lefkowicz AT, Wolpaw JR. Design and operation of an EEG-based brain–computer interface with digital signal processing technology. Behav Res Methods Instrum Comput 1997a; 29:337–45.
McFarland DJ, McCane LM, David SV, Wolpaw JR. Spatial filter selection for EEG-based communication. Electroenceph clin Neurophysiol 1997b;103:386–94.
Mima T, Hallett M. Corticomuscular coherence: a review. J Clin Neurophysiol 1999;16:501–11.
Niedermeyer E. The normal EEG of the waking adult. In: Niedermeyer E, Lopes da Silva F, editors. Electroencephalography: basic principles, clinical applications, and related fields. Philadelphia, PA: Lippincott Williams and Wilkins; 1999. p. 149–73.
Nunez PL. Localization of brain activity with electroencephalography. Adv Neurol 1990;54:39–65.
O'Donnell RD, Berkhout J, Adey WR. Contamination of scalp EEG spectrum during contraction of cranio-facial muscles. Electroenceph clin Neurophysiol 1974;37:145–51.
O'Dwyer NJ, Quinn PT, Guitar BE, Andrews G, Neilson PD. Procedures for verification of electrode placement in EMG studies of orofacial and mandibular muscles. J Speech Hear Res 1981;24: 273–88.
Panych LP, Wada JA, Beddoes MP. Practical digital filters for reducing EMG artefact in EEG seizure recordings. Electroenceph clin Neurophysiol 1989;72:268–76.
Pfurtscheller G, Neuper C, Guger C, Harkam W, Ramoser H, Schlogl A, Obermaier B, Pregenzer M. Current trends in Graz brain–computer interface (BCI) research. IEEE Trans Rehabil Eng 2000; 8:216–9.
Sadasivan PK, Dutt DN. Use of finite wordlength FIR digital filter structures with improved magnitude and phase characteristics for reduction of muscle noise in EEG signals. Med Biol Eng Comput 1995; 33:306–12.
Sasaki S, Iwata M. Immunocytochemical and ultrastructural study of the motor cortex in patients with lower motor neuron disease. Neurosci Lett 2000;281:45–8.
Scholle HCh, Scumann NP, Andres Ch, Mey E. Quantitative topographische Kennzeichnung myoelektrischer Aktivitätsverteilungen des M masseter: Mapping spektraler EMG-Parameter. EEG EMG Z Elektroenzephalogr Elektromyogr Verwandte Geb 1992;23: 115–20.
Srinivasan R, Nunez PL, Tucker DM, Silberstein RB, Cadusch PJ. Spatial sampling and filtering of EEG with spline Laplacians to estimate cortical potentials. Brain Topogr 1996;8:355–66.
Srinivasan R, Nunez PL, Silberstein RB. Spatial filtering and neocortical dynamics: estimates of EEG coherence. IEEE Trans Biomed Eng 1998; 45:814–26.
Sumitsuji N. EMG activities of facial muscles in resting state. Electromyogr Clin Neurophysiol 1986;26:555–6.
Van Boxtel A. Optimal signal bandwidth for the recording of surface, EMG activity of facial, jaw, and neck muscles. Psychophysiology 2001;38: 22–34.
Van Boxtel A, Goudswaard P, van der Molen GM, van den Sosch WEJ. Changes in electromyogram power spectra of facial and jaw-elevator muscles during fatigue. J Appl Physiol 1983;54:51–8.
Van Boxtel A, Goudswaard P, Schomaker LRB. Amplitude and bandwidth of the frontalis surface EMG: effects of electrode parameters. Psychophysiology 1984;21:699–707.
Willis J, Nelson A, Rice J, Black FW. The topography of muscle activity in quantitative EEG. Clin Electroencephalogr 1993;24:123–6.
Winter DA, Fuglevand AJ, Archer SE. Crosstalk in surface electromyography: theoretical and practical estimates. J Electromyogr Kinesiol 1994;4:15–26.
Wolpaw JR, Birbaumer N, Heetderks WJ, McFarland DJ, Peckham PH, Schalk G, Donchin E, Quatrano LA, Robinson CJ, Vaughan TM. Brain–computer interface technology: a review of the first international meeting. IEEE Trans Rehabil Eng 2000;8:164–73.
Wolpaw JR, Birbaumer N, McFarland DJ, Pfurtscheller G, Vaughan TM. Brain–computer interfaces for communication and control. Clin Neurophysiol 2002;113:767–91.
Wonnacott TH, Wonnacott R. Introductory statistics. New York, NY: Wiley; 1977.
Zafas H, Eriksson PO, North E, Al-Falahe N. Coordinated human jaw and head–neck movements during natural jaw opening–closing: reproducible movement patterns indicate linked motor control. In: Taylor A, Gladden MH, Durbaba R, editors. Alpha and gamma motor systems. New York, NY: Plenum Press; 1995. p. 502–4.